**ARTICLE**

BIOTECHNOLOGY BIOENGINEERING WILEY

# Omics analysis reveals mechanism underlying metabolic oscillation during continuous very-high-gravity ethanol fermentation by *Saccharomyces cerevisiae*

Xue Zhang[1] | Liang Wang[2] | Qian Li[3] | Riaan den Haan[4] | Fan Li[5] |
Chen-Guang Liu[1] | Feng-Wu Bai[1]

[1]State Key Laboratory of Microbial Metabolism, Joint International Research Laboratory of Metabolic & Developmental Sciences, School of Life Sciences and Biotechnology, Shanghai Jiao Tong University, Shanghai, China

[2]School of Biological Engineering, Dalian Polytechnic University, Dalian, Liaoning, China

[3]School of Life Science and Biotechnology, Dalian University, Dalian, Liaoning, China

[4]Department of Biotechnology, University of the Western Cape, Bellville, South Africa

[5]COFCO Nutrition & Health Research Institute, Beijing, China

**Correspondence**
Chen-Guang Liu, School of Life Sciences and Biotechnology, Shanghai Jiao Tong University, 800 Dongchuan Rd, 200240 Shanghai, China.
Email: cg.liu@sjtu.edu.cn

**Abstract**

During continuous very-high-gravity (VHG) ethanol fermentation with *Saccharomyces cerevisiae*, the process exhibits sustained oscillation in residual glucose, ethanol, and biomass, raising a question: how do yeast cells respond to this phenomenon? In this study, the oscillatory behavior of yeast cells was characterized through transcriptome and metabolome analysis for one complete oscillatory period. By analyzing the accumulation of 26 intracellular metabolites and the expression of 90 genes related to central carbon metabolism and stress response, we confirmed that the process oscillation was attributed to intracellular metabolic oscillation with phase difference, and the expression of *HXK1*, *HXT1,2,4*, and *PFK1* was significantly different from other genes in the Embden–Meyerhof–Parnas pathway, indicating that glucose transport and phosphorylation could be key nodes for regulating the intracellular metabolism under oscillatory conditions. Moreover, the expression of stress response genes was triggered and affected predominately by ethanol inhibition in yeast cells. This progress not only contributes to the understanding of mechanisms underlying the process oscillation observed for continuous VHG ethanol fermentation, but also provides insights for understanding unsteady state that might develop in other continuous fermentation processes operated under VHG conditions to increase product titers for robust production.

**KEYWORDS**
continuous ethanol fermentation, metabolomics, oscillation, transcriptomics, very-high-gravity

# 1 | INTRODUCTION

As global demand for crude oil further increases, diversification of fuel supply through exploring alternative energy sources such as fuel ethanol has become part of energy policies in many countries (Kircher, 2015). Although cellulosic ethanol is widely regarded as a promising liquid biofuel (Liu et al., 2019), a lack of substantial breakthrough in key technologies is still a major barrier for its implementation. Poor economic feasibility of this technology is a result of biomass pretreatment, generation of inhibitory compounds in the hydrolysate, high cost of cellulases and inefficient pentose assimilation by fermentation strains (Han et al., 2020). In addition, achievable cellulosic ethanol titers of only 5%–8% (v/v) are much lower than that of 12%–15% (v/v) for ethanol fermentation from starch-based feedstock, which significantly increases energy cost, particularly in downstream processes for ethanol distillation and stillage treatment (Bai et al., 2008).

Very-high-gravity (VHG) fermentation using sugars at concentrations higher than 25% (w/v) can produce ethanol as high as 15% (v/v) to save energy consumption for the whole process (Puligundla et al., 2011). However, VHG ethanol fermentation is usually practiced via labor-intensive and time-consuming batch operation, which is not suitable for large-scale production. Continuous VHG ethanol fermentation could be developed, but such a process often triggers sustained oscillation in residual glucose, ethanol concentration and biomass density, making it unsuitable for industrial production (Bai et al., 2009). Ethanol toxicity to *Saccharomyces cerevisiae* is a primary factor for triggering the process oscillation. Tolerance of yeast cells to ethanol toxicity is related to the fluidity, structure and composition of their plasma membrane as well as the level of unsaturated fatty acids, ergosterol, amino acids, inositol, heat shock proteins (HSPs), ATPase and storage carbohydrates (Lam et al., 2014).

Engineering strategies have been explored to attenuate process oscillation. For example: A stirred tank bioreactor followed by three cascade tubular bioreactors packed with Intalox ceramic saddles effectively alleviated ethanol inhibition in yeast cells, and consequently quasi-steady state was developed for the process (Bai, Chen, Anderson, et al., 2004). Stripping off ethanol directly from the fermentation broth by nitrogen gas or off-gas also attenuated the process oscillation (Wang et al., 2013). Kinetic models were also developed to characterize ethanol fermentation with different process states (Chen et al., 2005).

Periodic behavior has been investigated in eukaryotic and prokaryotic organisms (Panda, 2016). *S. cerevisiae* exhibits oscillatory behavior both in reactions catalyzed by cell-free extract and during continuous culture and fermentation (Bai et al., 2009; Chin et al., 2012) in the form of glycolytic oscillation with a period of about 1 min, respiratory oscillation with a period of 40−60 min, and cell cycle oscillation with a period of 2−45 h (Richard, 2003). The glycolytic oscillation is mediated by glycolytic intermediates, and phosphofructokinase (PFK) and its allosteric regulation were assumed to be responsible (Gustavsson et al., 2014; Olsen et al., 2020). The respiratory oscillation characterized by dissolved oxygen, oxygen uptake rate (OUR) and carbon dioxide evolution rate (CER) was modulated by sulfate assimilation, ethanol degradation, and respiration (Patnaik, 2003; Tu et al., 2007). The cell cycle oscillations, synchronized with the cell division cycle, were represented by extracellular parameters (OUR, CER, glucose, ethanol, and biomass), intracellular variables (storage carbohydrates) and cell cycle-related properties such as budding index and cell size (Ewald et al., 2016).

Although dynamic ethanol inhibition has been validated to be a key factor for triggering the process oscillation (Wang et al., 2013), how yeast cells respond remains a fundamental and unanswered question. In this study, a systematic approach via transcriptomic and metabolomic analysis was followed, with a focus particularly on the intracellular events of *S. cerevisiae* associated with the process oscillation under continuous VHG ethanol fermentation conditions.

# 2 | MATERIALS AND METHODS

## 2.1 | Strain, media, standards

All experiments were performed with the industrial yeast strain *S. cerevisiae* 4126 using YPD media composed of 5 g/L yeast extract, 3 g/L peptone and glucose at different concentrations. YPD media containing glucose of 30, 120, and 280 g/L were used for seed culture, pre-culture, and VHG fermentation, respectively. The media for seed culture and pre-culture were sterilized at 121°C for 20 min, but the VHG medium was sterilized at 110°C for 15 min to minimize the Maillard reaction. Yeast extract, peptone, and glucose were supplied by Sangon Biotech.

The following metabolites: G6P, F6P, FBP, 6PG, R5P, T6P, TRE, GAP, GOLP, G3P, PEP, PYR, OAA, CIT, AKG, SUC, FUM, MAL, ATP, ADP, AMP, NAD+, NADH, NADP+, NADPH andAcCoA used as standards for the LC-MS/MS analysis were purchased from Sigma-Aldrich.

## 2.2 | Pre-culture and continuous VHG ethanol fermentation

The slant yeast stock was inoculated into a 250 ml flask containing 100 ml seed medium, and cultured overnight at 30°C and 150 rpm, which was then inoculated into the fermenter (KoBioTech-2.5L) containing 1.6 L medium composed of 120 g/L glucose for a total working volume of 1.7 L. The pre-culture was performed at 30°C and 300 rpm with pH-controlled at 4.5 automatically by adding 2 M NaOH. Meanwhile, membrane-filtered air wassparged continuously into the fermenter at 85 ml/min, equivalent to 0.05 vvm, for micro-aeration conditions to stimulate yeast growth. When residual glucose in the pre-culture decreased to ~1.0 g/L, continuous VHG ethanol fermentation was initiated by feeding VHG medium at the dilution

rate of 0.027 h$^{-1}$, and temperature, rotating speed, pH, and aeration rate were same as that applied to the pre-culture. The process diagram is shown in Figure S1.

## 2.3 | Fermentation parameters determination

Fermentation parameters including residual glucose, ethanol, glycerol, biomass, cell viability and oxidation reduction potential (ORP) were measured to assess the continuous VHG ethanol fermentation system.

Triplicate samples, each with 5 ml, were centrifuged by Eppendorf 5810R at 10,000 rpm for 2 min, and the same centrifuge was used thereafter. Cell pellet was collected for biomass measurement, and the supernatant was frozen at −20°C temporarily for HPLC analysis. The HPLC system with RI-detector (Waters 410) and Aminex HPX 87-H column (300 × 7.8 mm; Bio-Rad Laboratories) was used to analyze glucose, ethanol, and glycerol in the fermentation broth according to the protocol developed previously by Wang et al. (2013). Biomass was characterized by dry cell weight (DCW) through washing the cell pellet twice with deionized water and drying overnight at 80°C to constant weight for balancing. Cell viability was evaluated via methylene blue stain described previously by Bai, Chen, Zhang, et al. (2004). Living cells were calculated through biomass × viability. ORP value was monitored by an ORP electrode.

## 2.4 | RNA extraction and analysis of extracellular metabolites

About 5 ml yeast cell suspension was sampled from the fermenter at designated time point, which was centrifuged at 10,000 rpm for 2 min. The supernatant was frozen at −20°C temporarily for analyzing extracellular metabolites, and the cell pellet was collected, washed with 0.9% (w/v) NaCl, and centrifuged again at 10,000 rpm for 2 min, which was then frozen immediately at −80°C for later RNA extraction.

Total RNA was extracted by the RNeasy Mini Kit (Qiagen). RNA quality was confirmed by $A_{260}/A_{280} > 2.0$ and agarose gel electrophoresis (28S/18S 1.5–2.0). RNA samples were dissolved in Milli-Q water and frozen at −80°C for transcriptome analysis at The Beijing Genomics Institute (BGI) Huada company.

## 2.5 | Transcriptomic analysis

High-resolution genome-wide transcription analysis was performed through RNA-Seq at Beijing Genomics Institute (BGI) Huada. Raw reads were filtered to remove some adapters and low-quality reads, and the remained reads were mapped to the reference genome S288c_reference_genome_R6-1-1_20110203 for transcript information. The gene expression was normalized by reads per kilobase per million mapped reads (RPKM), the number of reads per kilobase per

million mapped reads. Differentially expressed genes (DEGs) were defined as significantly upregulated or downregulated with the criteria of $-1.0 \geq \text{Log}_2 R \geq 1.0$ and false discovery rate (FDR) < 0.01, in which R is the fold change for the expression of same genes at time points investigated. In the analysis of the expression of stress-related genes, we collected the RPKM values for stress-related genes at each sampling point as a data set to perform paired difference test (t test) for their expression at different time points.

## 2.6 | Confirmation of transcriptomic analysis by quantitative real-time polymerase chain reaction (qRT-PCR)

qRT-PCR was performed to validate the transcriptomic analysis. Six genes, *ZPS1* (zinc regulatory proteins), *DSE1* (cell division), *HPF1* (mannose glycoprotein), *EGT2* (cell division), *TIS11* (iron regulatory proteins) and *GCV1* (synthesis of coenzyme factors), were selected for the qRT-PCR confirmation, and the primers used for their amplification are shown in Table S1.

## 2.7 | Quenching and extraction of intracellular metabolites

Approximately 5 ml suspension was sampled from the fermenter, which was mixed with 25 ml 60% (v/v) methanol solution precooled at −40°C for 3 min to quench yeast cell metabolism. The yeast cells were then collected by vacuum filtration through a 0.45 μm membrane, and the cake was washed with 5 ml 50% (v/v) methanol solution precooled at −40°C to remove impurities, which was then transferred rapidly into 9.5 ml precooled (−40°C) extraction solution composed of 2.5 ml methanol, 5 ml chloroform and 2 ml tricine-EDTA buffer solution (3 mmol/L tricine and 3 mmol/L EDTA at pH 7.0). The mixture was shaken for 50 min at −40 ± 5°C in a dry ice-ethanol bath. The supernatant was collected by centrifugation at 12,000 rpm and −19°C for 5 min, which was stored at −80°C before analyzing intracellular metabolites. Before the analysis was performed, the samples were de-frozen and evaporated to remove the solvent. The residue was dissolved into 100 μl of Mill-Q water for analysis by LC-MS/MS.

## 2.8 | LC-MS/MS analysis

The LC-MS/MS system included an HPLC (Thermo Fisher Scientific Inc.) with XBridge BEH Amide column (2.5 μm, 2.1 × 100 mm; Waters) operated at 25°C and a triple quadrupole mass spectrometer TSQ Quantum UltraTM (Thermo Fisher Scientific Inc.). The auto-sampler temperature was kept at 4°C, and 5 μl of sample was uploaded for the analysis. A gradient elution was applied using two eluents: eluent A was 20 mmol/L NH$_4$Ac in Milli-Q water, pH 6.5 and eluent B was 100% acetonitrile. The process was run at a flow rate of

0.3 ml/min, starting with 5% A, which was increased linearly to 60% in 20 min and maintained at 60% for 5 min, and then decreased to 5% A in 10 min. An equilibration time of 15 min was applied to the column for subsequent analysis.

Ionization was performed using an electrospray ionization (ESI) source operating at either positive or negative ionization mode. Nitrogen was used for both the sheath and the auxiliary gases and argon was used for collisionally induced dissociation. The software Xcalibur 2.2 was used for operating control and data acquisition. Selected reaction monitoring mode was used to eliminate signal noise, and the ionization mode with high efficiency of each metabolite was selected by the MS signal. Among 26 key metabolites, 18 of them (G6P, F6P, FBP, 6PG, R5P, T6P, TRE, GAP, GOLP, G3P, PEP, PYR, OAA, CIT, AKG, SUC, FUM, and MAL) presented ionization efficiency in the negative mode, and the others (ATP, ADP, AMP, $NAD^+$, NADH, $NADP^+$, NADPH, and AcCoA) presented ionization efficiency in the positive mode. The ESI spray voltage, vaporizer temperature, sheath gas pressure, collision pressure, and auxiliary gas pressure were 2.5 kV, 250°C, 35 psi, 1.5 psi, and 10 psi, respectively.

## 3 | RESULTS

### 3.1 | Physiology of *S. cerevisiae* in continuous VHG ethanol fermentation

During continuous VHG ethanol fermentation, the periodic oscillation of fermentation parameters, such as biomass, cell viability, ethanol, residual glucose and glycerol, was observed with a period of approximately 150 h at the dilution rate of $0.027 \, h^{-1}$ (Bai, Chen,

Anderson, et al., 2004; Wang et al., 2013). To focus on the intracellular regulation mechanism of yeast cells during the oscillatory process, a complete period is highlighted in Figure 1, in which ethanol, glycerol, biomass, cell viability, and the percentage of living cells exhibit similar oscillatory profiles, but residual glucose presents an opposite oscillation.

Due to their periodic and sinusoidal characteristics, phase differences were analyzed to characterize the oscillatory behaviors of these process parameters for better understanding of their correlations. We define the phase of a sine function with different patterns in a cycle (Figure S2). The oscillatory profile of residual glucose was designated with Phase 0 as the reference. As a result, the oscillatory profiles of ethanol and glycerol were characterized by a phase difference of π, and so were that for total biomass, cell viability and living cells, since yeast growth was coupled with the production of primary metabolites such as ethanol and glycerol. However, the change of yeast cell growth and viability (gradient) occurred before other process parameters, reflecting a lag response of intracellular metabolites to environmental changes. In addition, high glucose and ethanol simultaneously exerted on yeast cells caused a synergistic inhibition on their viability. Based on the biomass profile, 5 representative sampling points (P1−P5 in Figure 1) were selected for the subsequent metabolic profiling and transcriptomic analysis.

### 3.2 | Statistical analysis of DEGs

DEGs screened for the oscillation period based on the RNA transcription data are summarized in Figure 2. It is obvious that the intracellular transcriptional response of yeast cells at P1 is relatively
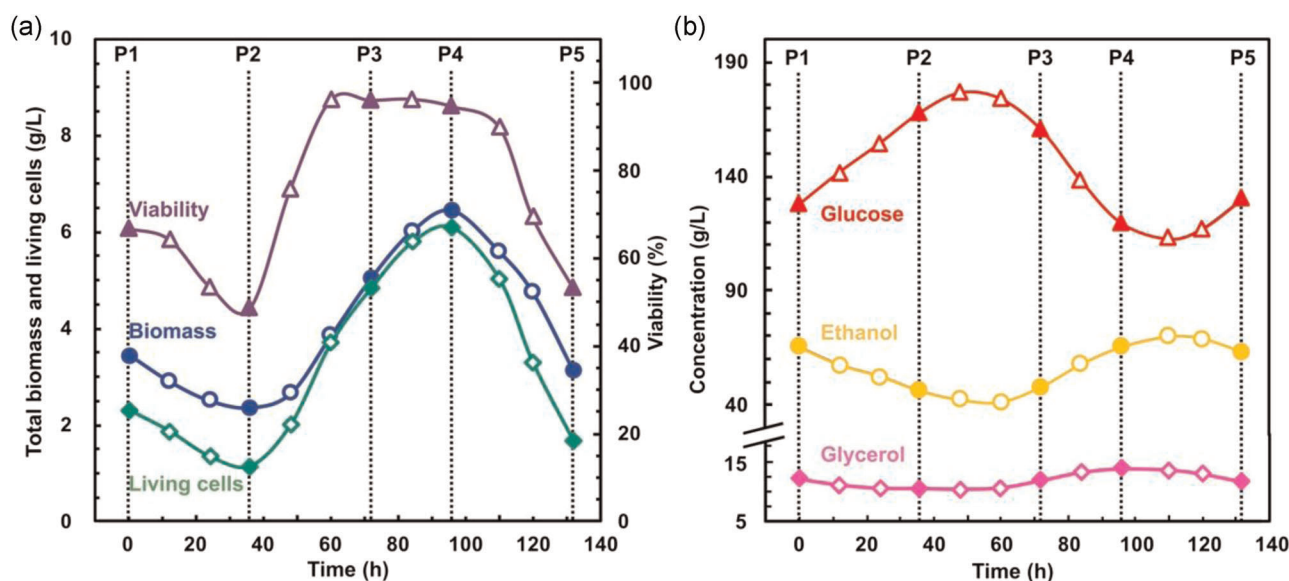


**FIGURE 1** (a) Profiles of total biomass, living cells, and cell viability and (b) residual glucose, ethanol, and glycerol in the fermentation broth as well as their phase differences in a complete oscillation period. P1−P5 represent time points for biomass sampling to explore intracellular response to the process oscillation [Color figure can be viewed at wileyonlinelibrary.com]
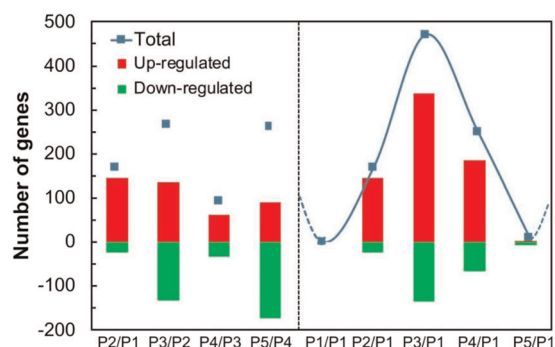
**FIGURE 2** Statistical analysis for DEGs selected with the threshold $-1 \geq \mathrm{Log}_2R \geq 1$ (R, fold change). Comparison between adjacent samples (left) and all samples to P1 (right). DEG, differentially expressed gene [Color figure can be viewed at wileyonlinelibrary.com]

consistent with that detected at P5 with only 10 DEGs screened, suggesting that yeast cells present similar transcriptional characteristics at the same phase points of different oscillation periods, and the end for a previous oscillation period represents the start for the next one.

More counts for DEGs between neighboring points indicate more significant transcriptional change associated with the unsteady state of continuous VHG ethanol fermentation. Compared to the initial status of yeast cells at P1, their total counts of DGEs at P2–P5 fit with the biomass profile through the phase difference of π. The most DEGs were observed at P3 due to the maximal phase difference between P3 and P1, or P5 that was equivalent to P1.

The qRT-PCR measurement for the expression of six selected genes indicates their upregulation from P1 to P2 to P3 and downregulation from P3 to P4 to P5, which are consistent with the results of their RNA-seq analysis, and thus verified the reliability of the transcriptome analysis (Figure S3).

## 3.3 | Intracellular metabolites and gene expression for central carbon metabolism

Cells are able to assess metabolic flux by fine tuning the rate of metabolic reactions, and consequently regulate intracellular physiology under stressful conditions (Litsios et al., 2018). During continuous VHG ethanol fermentation with glucose as the sole carbon source and ethanol, $CO_2$, biomass, and glycerol as major products and byproducts, the central carbon metabolism of yeast cells consists of the Embden–Meyerhof–Parnas (EMP) pathway, the pentose phosphate pathway (PPP) and the tricarboxylic acid cycle (TCA) (Figure S4). Thus, the metabolomics and transcriptomic data set of yeast cells was interpreted via pathway-based methods, referring to 26 metabolites and 90 genes related to central carbon metabolism, whose responses to the oscillation period are shown in Figure 3.

Glucose was metabolized predominantly through EMP to provide ATP and precursors for yeast growth, which composes of an energy-consuming phase (2 mol ATP/mol glucose consumed from GLC to GAP) and an energy-producing phase (4 mol ATP/mol glucose generated from GAP to PYR). PPP as sources for NADPH and pentose contains an oxidative pathway from G6P to Ri5P and a nonoxidative pathway from Ri5P to F6P and GAP. TCA includes a series
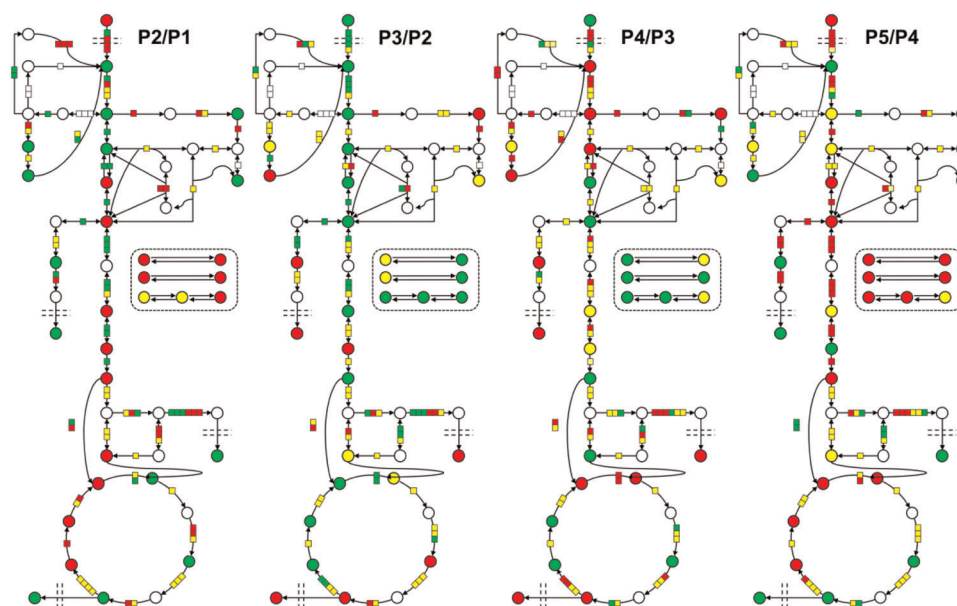


**FIGURE 3** Overview for the metabolome and transcriptome of central carbon metabolism for samples collected at adjacent time points. The gene expression and metabolite pool were marked by rectangles/squares and circles, respectively. Red, green, and yellow represented upregulation, downregulation, and no significant change between the two samples. Refer to Figure S4 for more details of the metabolites and enzymes [Color figure can be viewed at wileyonlinelibrary.com]

of enzyme-catalyzed reactions for aerobic respiration in yeast cells. For continuous VHG ethanol fermentation, central carbon metabolism of *S. cerevisiae* was weakened from P2 to P3, especially for EMP and TCA, but enhanced from P3 to P4 to P5 as more glucose metabolized and ethanol increased.

Figure 4a shows intracellular accumulation of metabolites involved in the central carbon metabolism and their profiles within the oscillation period. ATP was the dominant intracellular adenine nucleotide, and the energy charge (EC = [ATP] + 0.5 × [ADP]/[ATP] + [ADP] + [AMP]) was higher than 0.9, indicating that yeast cells had a strong potential for phosphoryl transfer to support active metabolism (Guimaraes & Londesborough, 2008). Moreover, we noticed that the profile of EC is identical to that observed for the total biomass (Figure 1), since the growth of yeast cells was energy-consuming.

With the oscillation of glucose as the reference (Phase 0), most profiles for intracellular accumulation of metabolites and expression of DEGs can be fitted into sine function with Phase 0, π/2, π and 3π/2, respectively (Figure S2). While the expression of 16 genes in 22 genes related to the EMP pathway is with Phase π/2, the expression of another five genes (*HXK1*, *HXT1,2,4*, and *PFK1*) is with Phase 3π/2, 0 and π, respectively, indicating glucose transport and phosphorylation as well as further phosphorylation of F6P catalyzed by PFK could be key nodes for regulating the oscillation of intracellular metabolites (Figure 4b). While the oscillatory profiles of G6P and F6P that are upstream of the phosphorylation catalyzed by PFK are with Phase π/2, the profiles of FBP and GAP that are downstream of the reaction are with Phase 0, and the phase difference of π/2 is assumed to be induced by the activity of PFK to convert F6P to FBP, indicating that PFK is the key rate-limiting enzyme in the energy-consuming phase of the glycolytic pathway. This is similar to the mechanism underlying oscillation associated with continuous culture of *S. cerevisiae* and the enzymatic reactions catalyzed by extracts of the yeast (Boiteux et al., 1975; Papagiannakis et al., 2017; Thoke et al., 2018).

For ethanol production downstream of the EMP pathway, the expression of *ADH4* was vigorous, peaking at P3 with a RPKM value of 4300 with Phase π/2, but the expression of *PDC1* and *ADH1* was with Phase 3π/2, which is consistent with the expression of most genes in the EMP pathway, but presents a phase difference of π with the expression of *PDC5,6* and *ADH4* (Figure 4b). The expression profiles of *ADH4* and *PDC5* are earlier than ethanol with a phase difference of π/2, but the expression level of *ADH4* is much higher than that of *PDC5*, suggesting that Adh4p might be responsible for ethanol formation during continuous VHG ethanol fermentation. The gene *ADH4* encodes a zinc-dependent alcohol dehydrogenase isoenzyme, and its transcription is induced in response to zinc deficiency, which is consistent with the expression profile of *ZPS1*, a gene related to zinc deficiency (Figure S3).

The yeast cells produced 10.2–13.7 g/L glycerol during continuous VHG ethanol fermentation, and the oscillatory profile of glycerol shows a pattern of Phase π, presenting a phase inversion to

that of *HOR2* as well as to the ORP profile (Figure S5). We also found that there is a phase difference of π between the oscillation of glycerol (Figure 1b) and the expression of *GDP1* (Figure 4b). The expression of *GPD1* and *GPD2* are regulated by osmotic stress and redox homeostasis, and studies have shown that the HOG pathway where the *GPD1* and *GPD2* are located can respond to ethanol stress (Klein et al., 2017; Udom et al., 2019), suggesting that glycerol production during continuous VHG ethanol fermentation might be induced collectively by osmotic stress, ethanol inhibition, and the redox environment.

The expression of genes related to PPP is far below that of genes in the EMP pathway, indicating that intracellular anabolism might be repressed during continuous VHG ethanol fermentation. The oxidation stage of the PPP pathway is from G6P to 6PG, and finally to Ri5P, and both generate NADPH, which provides reducing power and precursor metabolites for the biosynthesis of yeast cells. The oscillation of 6PG is with Phase π, similar to that of the total biomass (Figure 1), indicating that yeast growth is closely related to the generation of NADPH. Furthermore, the expression of *ALD4*, *ALD6*, *MAE1* (Figure S6) and *ADH4* exhibits a phase of 3π/2, ahead of the intracellular accumulation of NADH and NADPH. The products of *ALD4*, *ALD6* and *MAE1* are involved in catalyzing the generation of NAD(P)H, suggesting that the cofactor might be the driving force for the PPP pathway and biomass accumulation.

Continuous VHG ethanol fermentation was conducted under microaeration conditions. As a result, flux to the TCA cycle should be low, and the transcriptional analysis confirmed such a speculation, since the expression of genes related to the TCA cycle is much lower than that related to the EMP pathway.

## 3.4 | Dynamic expression of genes associated with stress response

Yeast cells suffer from multiple stresses during continuous VHG ethanol fermentation such as ethanol inhibition, osmotic pressure from glucose and redox stress associated with imbalanced energy metabolism (Auesukaree, 2017; Burphan et al., 2018; Caspeta et al., 2015), and metabolism of storage carbohydrates including trehalose, glycogen, and glycan has been investigated to help determine their impact on yeast cells (Babazadeh et al., 2017; Li et al., 2009). During the oscillation, significant changes were detected in the expression of genes related to stress response, in particular the transcription of genes responded to oxidative stress.

Figure 5 shows the transcription profiles of genes responding to oxidative stress, and most of them were overexpressed at P4 with the one-tailed *p* value of .024 for the paired samples between P4 and P3. For ethanol fermentation, major stresses on yeast cells are from ethanol inhibition and osmotic pressure exerted by glucose. Since glucose decreased from P3 to P4 for less osmotic stress, but ethanol increased to exert more severe inhibition on yeast cells, we conclude that ethanol inhibition would be the major stress on yeast cells
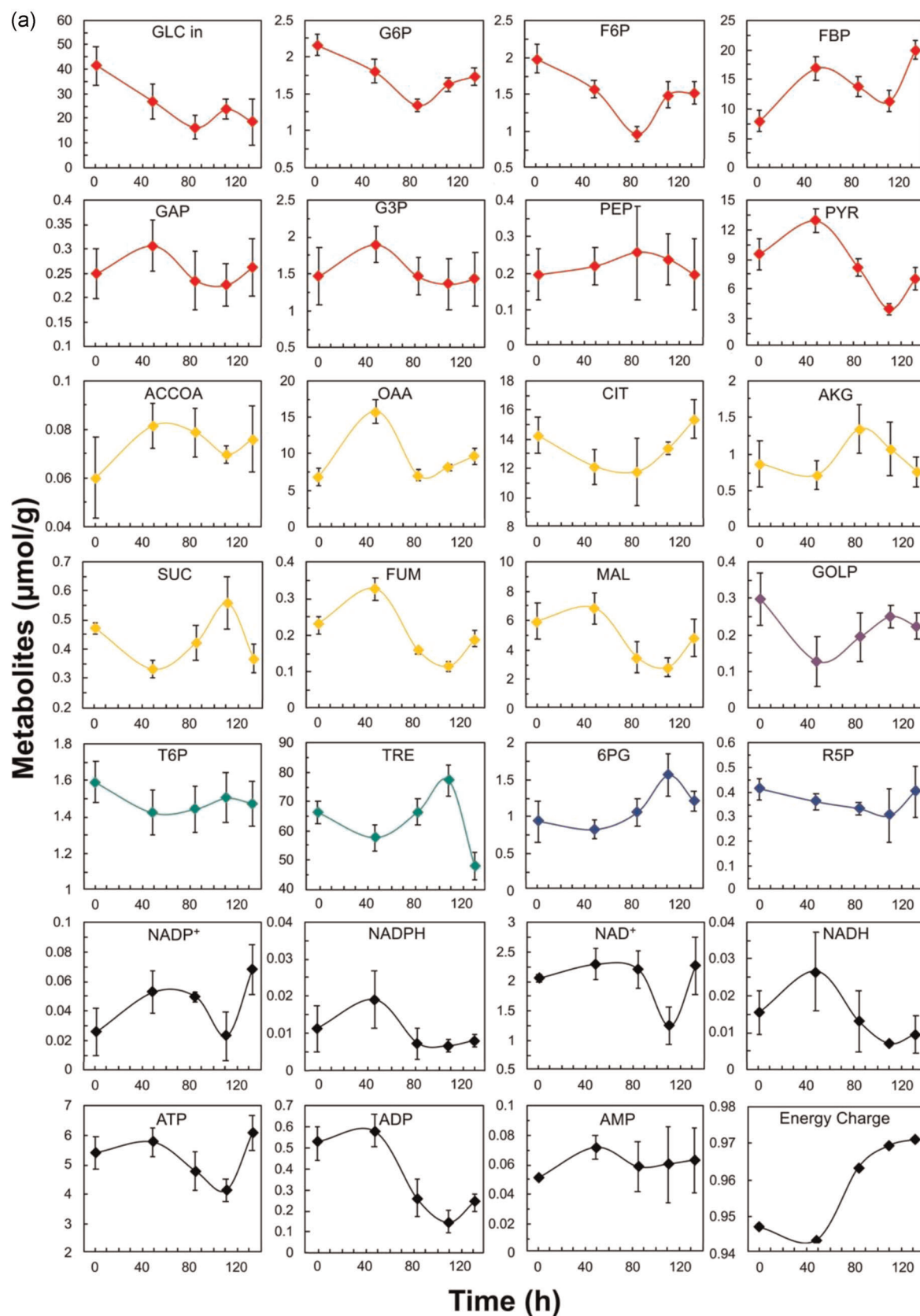
**FIGURE 4** (a) Intracellular metabolites and (b) the expression of genes in an oscillation period. Major pathways for carbon metabolism such as glycolysis (red), ethanol production (pink), TCA (yellow), glycerol production (purple), trehalose synthesis (green), PPP (blue), and other related factors (black) were targeted for the analysis. PPP, pentose phosphate pathway; TCA, tricarboxylic acid cycle [Color figure can be viewed at wileyonlinelibrary.com]
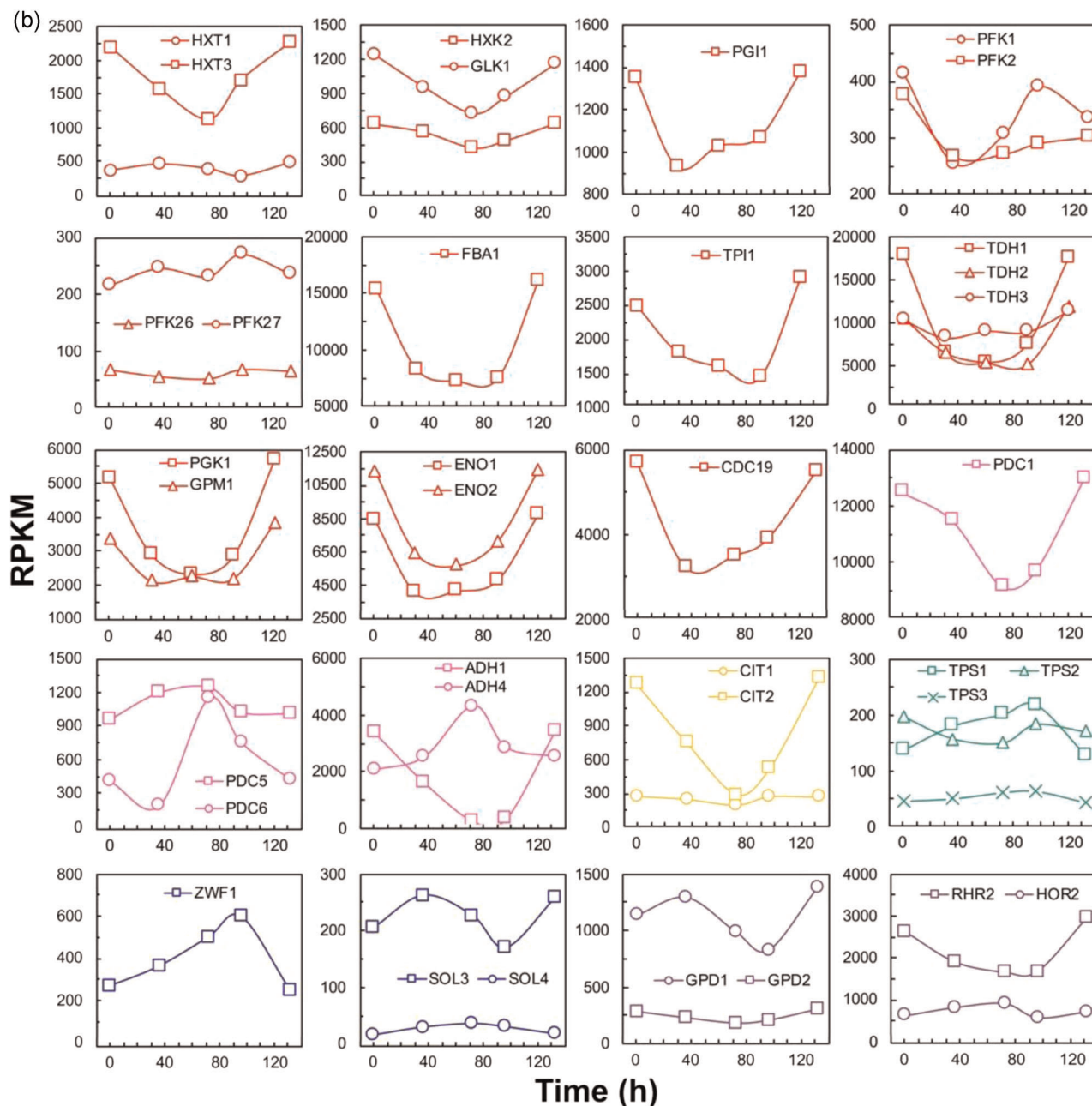
**FIGURE 4** Continued

during oscillation observed under continuous VHG fermentation conditions.

HSPs are a highly conserved family of molecular chaperones that play a key role in the correct transport, assembly, and folding of proteins (Mühlhofer et al., 2019). Due to the synergistic effect of multiple stresses during continuous VHG ethanol fermentation, the upregulation of HSPs is observed. *HSP10* and *HSP60* are molecular chaperones to help correct misfolding of proteins in mitochondrial matrix including ATPases (Hipp et al., 2019), which cooperates with each other so that their expression profiles are similar. *HSP26* and *HSP42* are small heat shock proteins that form oligomers to suppress

unfolded protein aggregation under stressful conditions (Franzmann et al., 2008), which were also differentially expressed. The expression of these HSPs is consistent with changes in ethanol concentration, indicating that cellular protein denaturation might be predominately triggered by ethanol inhibition. Although the expression of *HSP31* was much higher at P4, no significant difference was observed between P3 and P4, indicating its role in responding to ethanol stress faster than others.

In addition, it seems that the oscillation of ethanol concentration was mainly responsible for the expression response of *SOD1*. During continuous VHG ethanol fermentation,
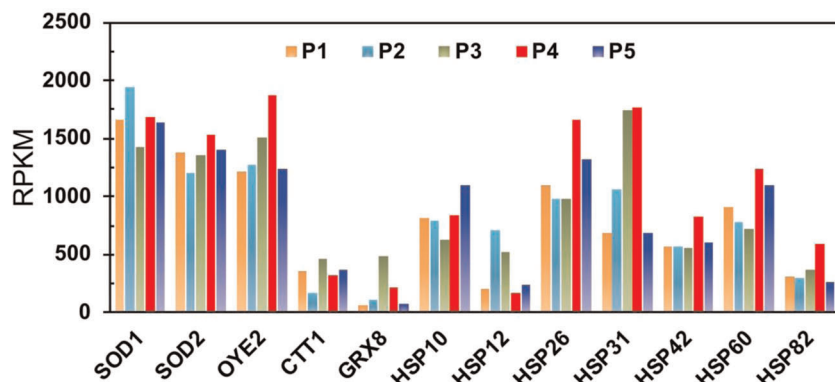
**FIGURE 5** Expression of genes related to stress responses, which has a significant difference between P3 and P4 (paired samples $t$ tests, one-tailed $p$ value = .024 < .05) [Color figure can be viewed at wileyonlinelibrary.com]

*S. cerevisiae* experienced stress from intracellular reactive oxygen species (ROS), and consequently oxidative damage to its cell structures. Superoxide dismutases (SODs), the major ROS-scavenging enzymes, are classified into two groups based on their subcellular localization and demand for metal cofactors, namely cytosolic Cu/Zn-SOD (Sod1p) and mitochondrial Mn-SOD (Sod2p) (Culotta et al., 2006). Although both *SOD1* and *SOD2* were overexpressed in the whole oscillation for tolerance to ROS stress, the expression of *SOD1* was 21.6% higher than that of *SOD2*, which might be due to ethanol production in the cytoplasm for ROS stress.

*OYE2* encoding NADPH dehydrogenase is another gene responding to oxidative stress (Partow et al., 2017), which was overexpressed at P4 to address redox imbalance. On the other hand, the expression of two oxidative stress-related genes, *CTT1* encoding cytosolic catalase (Martins & English, 2014) and *GRX8* encoding glutathione-disulfide reductase (Tang et al., 2014), were much lower within the complete oscillation period, probably due to their weak role in responding to stresses exerted by ethanol inhibition and osmotic pressure from glucose as well.

Moreover, when the expression of these oxidative stress-responding genes was compared between P1 and P5, no significant difference was observed, indicating that oscillation also occurred in their expression and intracellular metabolism.

## 3.5 | Dynamics of gene expression associated with anabolism

Biomass density as an important process parameter oscillated periodically in continuous VHG ethanol fermentation, indicating that anabolism of yeast cells might also experience oscillation. Transcriptome analysis indicated that a large number of genes related to ribosome synthesis were expressed in a periodic pattern. As shown in Figure 6, most DEGs were upregulated from P1 to P2 and P4 to P5/P1, but downregulated from P3 to P4, but no significant difference was observed at P2 and P3. As a result, the expression of genes related to ribosome synthesis oscillated with Phase 0, indicating that ribosome synthesis was robust from P1 to P2 to P3 and P4 to P5/P1, but not active from P3 to P4.

The upregulated expression of genes related to ribosome synthesis symbolizes starting of anabolic metabolism. Thus, it can be speculated that yeast cell anabolism was initiated at P4 with the lowest transcription of genes related to ribosome synthesis, and the process continued to next oscillation period from P4 to P5/P1 to P2. While oscillation for biomass density presented with Phase π, which was later than the ribosome synthesis for a phase difference of π, the increased expression of ribosomal genes before the biomass accumulation indicated that ribosome synthesis was a preparation for yeast growth under stressful conditions. In addition, oscillation in the expression of ribosomal synthesis gene is opposite in phase to that for ethanol concentration with a phase difference of π, which might suggest that regulation on the expression of ribosomal synthesis genes was also related to ethanol stress.

## 4 | DISCUSSION

Among stresses that yeast cells encounter during VHG ethanol fermentation, dynamic ethanol inhibition was recognized as a major factor for triggering the process oscillation, and the critical ethanol concentration $E_{crit}$ of ~ 50 g/L was experimentally observed for significant inhibition in yeast growth to trigger the process oscillation (Wang et al., 2013). When ethanol concentration exceeded $E_{crit}$, yeast growth was inhibited significantly, and consequently biomass density decreased, since yeast cells were being discharged out of the fermenter continuously. However, yeast cells within the fermenter still produced ethanol vigorously, and ethanol concentration kept increasing for a while till ethanol produced was less than ethanol discharged with the fermentation broth under the dilution rate applied to the continuous VHG ethanol fermentation system, making the time for ethanol to increase to its maximum later than that for biomass to approach to its highest level (Figure 1). Therefore, sustained oscillation under continuous VHG ethanol fermentation is collectively contributed by yeast growth, ethanol production and inhibition in yeast growth.

The concentration of intracellular metabolites in the EMP pathway also oscillated, but a phase difference of π/2 was observed for those with energy consumption and production. The generation of such an oscillation behavior might be from the phosphorylation reaction catalyzed by PFK. *PFK1* and *PFK2* encode the 4α and 4β
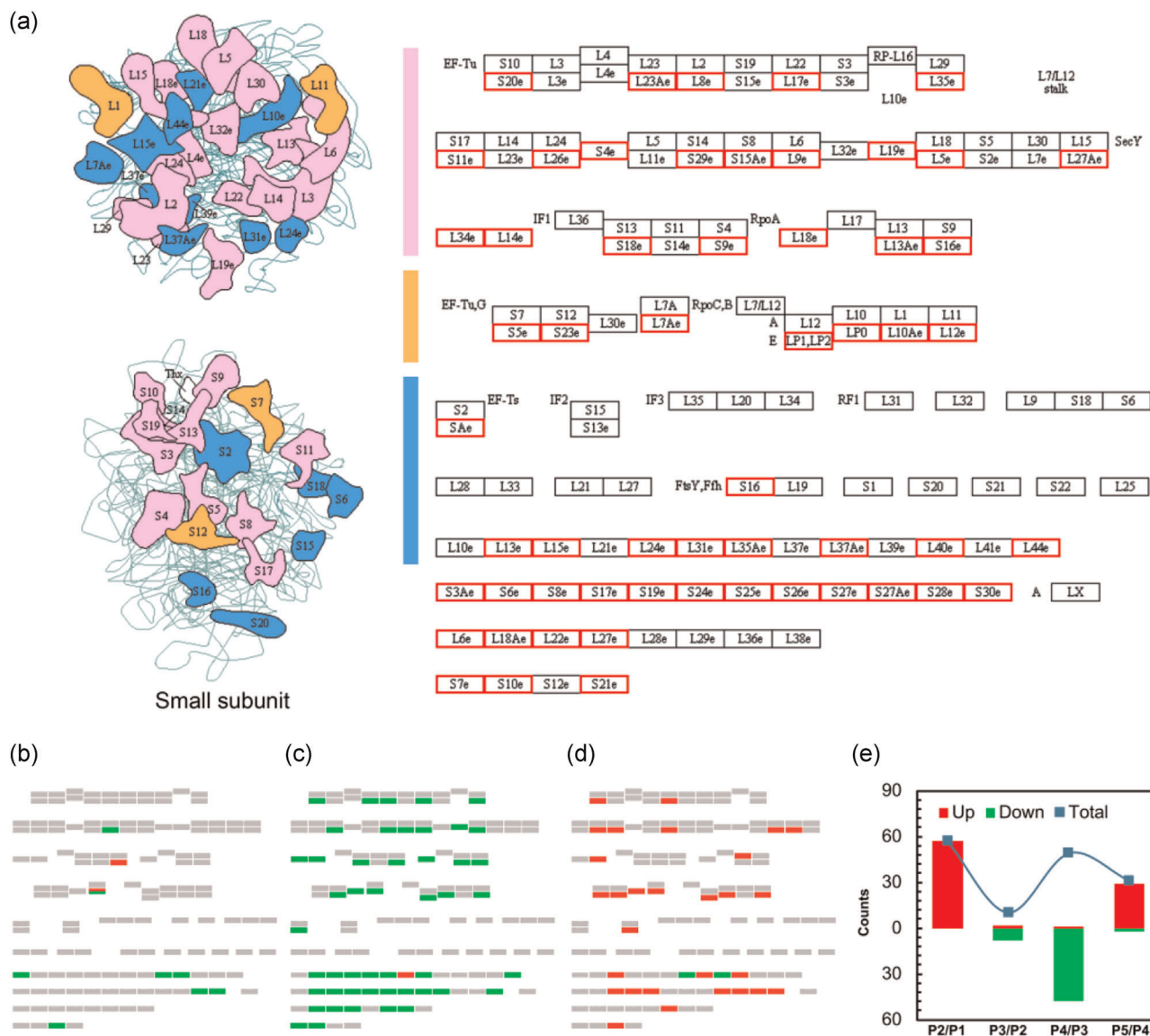
**FIGURE 6** Analysis of DEGs in the synthesis of ribosome subunits. The DEGs between (a) P2/P1, (b) P3/P2, (c) P4/P3, (d) P5/P4, and (e) the total counts. DEG, differentially expressed gene [Color figure can be viewed at wileyonlinelibrary.com]

subunits of the heterooctameric enzyme in yeast for the activity of PFK (Heinisch et al., 1996). It's interesting that unlike *PFK1*, *PFK2* was not substantially induced from P2 to P3 to P4 (Figure 4b), indicating that *PFK1* was upregulated more significantly than *PFK2* in response to the increase of glucose concentration.

On the other hand, PFK activity is also subject to allosteric regulation: inhibited by ATP, but activated by AMP (Heinisch et al., 1996) and ADP (Zheng, Liu, Sun, Wu, & He, 2017). Therefore, the oscillation of intracellular ATP with Phase 0 was characterized by a phase inversion compared to that for the expression of *PFK1* with Phase π, reflecting its allosteric regulation on PFK, but the oscillation of intracellular AMP was different from ATP, probably because its oscillation amplitude was much lower than that of ATP, making its regulation less significant.

According to the results in Figure 4b, the expression of *ADH1* and *PDC1* was consistent with that for most genes of the EMP pathway, but the expression of *ADH4*, *PDC5*, and *PDC6* was different. It is speculated that regulation on the expression of *ADH1* and *PDC1* is closely related to the metabolic flux for catabolism, but regulation on the expression of *ADH4*, *PDC5*, and *PDC6* is more related to the metabolic flux for anabolism.

Glycerol is formed in response to osmotic stress for intracellular redox homeostasis (Udom et al., 2019), but the flux of the TCA cycle is not significant under microaeration conditions employed to VHG ethanol fermentation. Meanwhile, genes for oxidative stress response, particularly those encoding the HSPs family proteins, were differentially expressed during continuous VHG ethanol fermentation, triggered mainly by ethanol inhibition.

Ethanol is a primary metabolite, and its production is tightly coupled with the growth of yeast cells through anabolic metabolism. Genes responsible for anabolic metabolism need to be upregulated before biomass accumulation. However, under stressful conditions associated with VHG ethanol fermentation, such a biosynthetic process is initiated from stress sensing, expression of related genes, to synthesis of proteins and many other metabolites, and phase differences have been observed on some of these events, suggesting a necessity for time delay in the biological process for yeast growth. As a result, we propose a mechanism underlying the process oscillation: a synergetic effect from the growth of yeast cells and their production of ethanol and response to ethanol inhibition.

## 5 | CONCLUSIONS

Continuous VHG ethanol fermentation using concentrated sugars for high ethanol titers not only saves energy consumption for ethanol distillation, but also reduces stillage discharge to save even more energy consumption for stillage treatment, but yeast cells inevitably experience various stresses, particularly ethanol inhibition that can trigger oscillation, making the process unsuitable for industrial production. Analysis on intracellular accumulation of metabolites associated with the central carbon metabolism of yeast cells and differential expression of genes encoding key enzymes and responding to environmental stresses confirmed their oscillations with phase differences for time delay. The enhancement of yeast tolerance to ethanol inhibition would help attenuate the process oscillation. Moreover, engineering other related metabolic pathways of yeast cells would be an alternative strategy for such a purpose to make continuous VHG ethanol fermentation at quasi-steady state, and thus suitable for industrial production.

### AUTHOR CONTRIBUTIONS

Xue Zhang: *data curation, formal analysis, writing, visualization*; Liang Wang: *investigation, writing—original draft, data curation*; Qian Li: *investigation, data curation*; Riaan den Haan: *writing—review and editing*; Fan Li: *methodology, resources*; Feng-Wu Bai: *funding acquisition, project administration, writing—review & editing*; Chen-Guang Liu: *conceptualization, supervision, data curation, writing—review and editing*.

### DATA AVAILABILITY STATEMENT

The data that support the findings of this study are available from the corresponding author upon reasonable request.

### ORCID

*Liang Wang* 🆔 https://orcid.org/0000-0002-3740-6421
*Chen-Guang Liu* 🆔 http://orcid.org/0000-0003-0343-6304
*Feng-Wu Bai* 🆔 http://orcid.org/0000-0003-1431-4839

### REFERENCES

Auesukaree, C. (2017). Molecular mechanisms of the yeast adaptive response and tolerance to stresses encountered during ethanol fermentation. *Journal of Bioscience and Bioengineering, 124*(2), 133–142. https://doi.org/10.1016/j.jbiosc.2017.03.009

Babazadeh, R., Lahtvee, P. J., Adiels, C. B., Goksor, M., Nielsen, J. B., & Hohmann, S. (2017). The yeast osmostress response is carbon source dependent. *Scientific Reports, 7*(1), 990. https://doi.org/10.1038/s41598-017-01141-4

Bai, F. W., Anderson, W. A., & Moo-Young, M. (2008). Ethanol fermentation technologies from sugar and starch feedstocks. *Biotechnology Advances, 26*(1), 89–105. https://doi.org/10.1016/j.biotechadv.2007.09.002

Bai, F. W., Chen, L. J., Anderson, W. A., & Moo-Young, M. (2004). Parameter oscillations in a very high gravity medium continuous ethanol fermentation and their attenuation on a multistage packed column bioreactor system. *Biotechnology and Bioengineering, 88*(5), 558–566. https://doi.org/10.1002/bit.20221

Bai, F. W., Chen, L. J., Zhang, Z., Anderson, W. A., & Moo-Young, M. (2004). Continuous ethanol production and evaluation of yeast cell lysis and viability loss under very high gravity medium conditions. *Journal of Biotechnology, 110*(3), 287–293. https://doi.org/10.1016/j.jbiotec.2004.01.017

Bai, F. W., Ge, X. M., Anderson, W. A., & Moo-Young, M. (2009). Parameter oscillation attenuation and mechanism exploration for continuous VHG ethanol fermentation. *Biotechnology and Bioengineering, 102*(1), 113–121. https://doi.org/10.1002/bit.22043

Boiteux, A., Goldbeter, A., & Hess, B. (1975). Control of oscillating glycolysis of yeast by stochastic, periodic, and steady source of substrate: A model and experimental study. *Proceedings of the National Academy of Sciences of the United States of America, 72*(10), 3829–3833. https://doi.org/10.1073/pnas.72.10.3829

Burphan, T., Tatip, S., Limcharoensuk, T., Kangboonruang, K., Boonchird, C., & Auesukaree, C. (2018). Enhancement of ethanol production in very high gravity fermentation by reducing fermentation-induced oxidative stress in *Saccharomyces cerevisiae*. *Scientific Reports, 8*(1), 13069. https://doi.org/10.1038/s41598-018-31558-4

Caspeta, L., Castillo, T., & Nielsen, J. (2015). Modifying yeast tolerance to inhibitory conditions of ethanol production processes. *Frontiers in Bioengineering and Biotechnology, 3*, 184. https://doi.org/10.3389/fbioe.2015.00184

Chen, L. J., Xu, Y. L., Bai, F. W., Anderson, W. A., & Moo-Young, M. (2005). Observed quasi-steady kinetics of yeast cell growth and ethanol formation under very high gravity fermentation condition. *Biotechnology and Bioprocess Engineering, 10*(2), 115–121.

Chin, S. L., Marcus, I. M., Klevecz, R. R., & Li, C. M. (2012). Dynamics of oscillatory phenotypes in *Saccharomyces cerevisiae* reveal a network of genome-wide transcriptional oscillators. *FEBS Journal, 279*(6), 1119–1130. https://doi.org/10.1111/j.1742-4658.2012.08508.x

Culotta, V. C., Yang, M., & O'Halloran, T. V. (2006). Activation of superoxide dismutases: Putting the metal to the pedal. *Biochimica et Biophysica Acta/General Subjects, 1763*(7), 747–758. https://doi.org/10.1016/j.bbamcr.2006.05.003

Ewald, J. C., Kuehne, A., Zamboni, N., & Skotheim, J. M. (2016). The yeast cyclin-dependent kinase routes carbon fluxes to fuel cell cycle progression. *Molecular Cell, 62*(4), 532–545. https://doi.org/10.1016/j.molcel.2016.02.017

Franzmann, T. M., Menhorn, P., Walter, S., & Buchner, J. (2008). Activation of the chaperone Hsp26 is controlled by the

rearrangement of its thermosensor domain. *Molecular Cell*, 29(2), 207–216. https://doi.org/10.1016/j.molcel.2007.11.025

Guimaraes, P. M., & Londesborough, J. (2008). The adenylate energy charge and specific fermentation rate of brewer's yeasts fermenting high- and very high-gravity worts. *Yeast*, 25(1), 47–58. https://doi.org/10.1002/yea.1556

Gustavsson, A. K., van Niekerk, D. D., Adiels, C. B., Kooi, B., Goksor, M., & Snoep, J. L. (2014). Allosteric regulation of phosphofructokinase controls the emergence of glycolytic oscillations in isolated yeast cells. *FEBS Journal*, 281(12), 2784–2793. https://doi.org/10.1111/febs.12820

Han, C., Yang, R., Sun, Y., Liu, M., Zhou, L., & Li, D. (2020). Identification and characterization of a novel hyperthermostable bifunctional cellobiohydrolase- xylanase enzyme for synergistic effect with commercial cellulase on pretreated wheat straw degradation. *Frontiers in Bioengineering and Biotechnology*, 8, 296. https://doi.org/10.3389/fbioe.2020.00296

Heinisch, J. J., Boles, E., & Timpel, C. (1996). A yeast phosphofructokinase insensitive to the allosteric activator fructose 2,6-bisphosphate. Glycolysis/metabolic regulation/allosteric control. *Journal of Biological Chemistry*, 271(27), 15928–15933. https://doi.org/10.1074/jbc.271.27.15928

Hipp, M. S., Kasturi, P., & Hartl, F. U. (2019). The proteostasis network and its decline in ageing. *Nature Reviews Molecular Cell Biology*, 20(7), 421–435. https://doi.org/10.1038/s41580-019-0101-y

Kircher, M. (2015). Sustainability of biofuels and renewable chemicals production from biomass. *Current Opinion in Chemical Biology*, 29, 26–31. https://doi.org/10.1016/j.cbpa.2015.07.010

Klein, M., Swinnen, S., Thevelein, J. M., & Nevoigt, E. (2017). Glycerol metabolism and transport in yeast and fungi: Established knowledge and ambiguities. *Environmental Microbiology*, 19(3), 878–893. https://doi.org/10.1111/1462-2920.13617

Lam, F. H., Ghaderi, A., Fink, G. R., & Stephanopoulos, G. (2014). Biofuels. Engineering alcohol tolerance in yeast. *Science*, 346(6205), 71–75. https://doi.org/10.1126/science.1257859

Li, L., Ye, Y., Pan, L., Zhu, Y., Zheng, S., & Lin, Y. (2009). The induction of trehalose and glycerol in *Saccharomyces cerevisiae* in response to various stresses. *Biochemical and Biophysical Research Communications*, 387(4), 778–783. https://doi.org/10.1016/j.bbrc.2009.07.113

Litsios, A., Ortega, A. D., Wit, E. C., & Heinemann, M. (2018). Metabolic-flux dependent regulation of microbial physiology. *Current Opinion in Microbiology*, 42, 71–78. https://doi.org/10.1016/j.mib.2017.10.029

Liu, C. G., Xiao, Y., Xia, X. X., Zhao, X. Q., Peng, L., Srinophakun, P., & Bai, F. W. (2019). Cellulosic ethanol production: Progress, challenges and strategies for solutions. *Biotechnology Advances*, 37(3), 491–504. https://doi.org/10.1016/j.biotechadv.2019.03.002

Martins, D., & English, A. M. (2014). Catalase activity is stimulated by H(2)O(2) in rich culture medium and is required for H(2)O(2) resistance and adaptation in yeast. *Redox Biology*, 2, 308–313. https://doi.org/10.1016/j.redox.2013.12.019

Mühlhofer, M., Berchtold, E., Stratil, C. G., Csaba, G., Kunold, E., Bach, N. C., Sieber, S. A., Haslbeck, M., Zimmer, R., & Buchner, J. (2019). The heat shock response in yeast maintains protein homeostasis by chaperoning and replenishing proteins. *Cell Reports*, 29(13), 4593–4607. https://doi.org/10.1016/j.celrep.2019.11.109

Olsen, L. F., Stock, R. P., & Bagatolli, L. A. (2020). Glycolytic oscillations and intracellular K(+) concentration are strongly coupled in the yeast *Saccharomyces cerevisiae*. *Archives of Biochemistry and Biophysics*, 681, 108257. https://doi.org/10.1016/j.abb.2020.108257

Panda, S. (2016). Circadian physiology of metabolism. *Science*, 354(6315), 1008–1015. https://doi.org/10.1126/science.aah4967

Papagiannakis, A., Niebel, B., Wit, E. C., & Heinemann, M. (2017). Autonomous metabolic oscillations robustly gate the early and late cell cycle. *Molecular Cell*, 65(2), 285–295. https://doi.org/10.1016/j.molcel.2016.11.018

Partow, S., Hyland, P. B., & Mahadevan, R. (2017). Synthetic rescue couples NADPH generation to metabolite overproduction in *Saccharomyces cerevisiae*. *Metabolic Engineering*, 43, 64–70. https://doi.org/10.1016/j.ymben.2017.08.004

Patnaik, P. R. (2003). Oscillatory metabolism of *Saccharomyces cerevisiae*: An overview of mechanisms and models. *Biotechnology Advances*, 21(3), 183–192. https://doi.org/10.1016/S0734-9750(03)00022-3

Puligundla, P., Smogrovicova, D., Obulam, V. S., & Ko, S. (2011). Very high gravity (VHG) ethanolic brewing and fermentation: A research update. *Journal of Industrial Microbiology & Biotechnology*, 38(9), 1133–1144. https://doi.org/10.1007/s10295-011-0999-3

Richard, P. (2003). The rhythm of yeast. *FEMS Microbiology Reviews*, 27(4), 547–557. https://doi.org/10.1016/S0168-6445(03)00065-2

Tang, Y., Zhang, J., Yu, J., Xu, L., Wu, J., Zhou, C. Z., & Shi, Y. (2014). Structure-guided activity enhancement and catalytic mechanism of yeast grx8. *Biochemistry*, 53(13), 2185–2196. https://doi.org/10.1021/bi401293s

Thoke, H. S., Olsen, L. F., Duelund, L., Stock, R. P., Heimburg, T., & Bagatolli, L. A. (2018). Is a constant low-entropy process at the root of glycolytic oscillations? *Journal of Biological Physics*, 44(3), 419–431. https://doi.org/10.1007/s10867-018-9499-2

Tu, B. P., Mohler, R. E., Liu, J. C., Dombek, K. M., Young, E. T., Synovec, R. E., & McKnight, S. L. (2007). Cyclic changes in metabolic state during the life of a yeast cell. *Proceedings of the National Academy of Sciences of the United States of America*, 104(43), 16886–16891. https://doi.org/10.1073/pnas.0708365104

Udom, N., Chansongkrow, P., Charoensawan, V., & Auesukaree, C. (2019). Coordination of the cell wall integrity and high-osmolarity glycerol pathways in response to ethanol stress in *Saccharomyces cerevisiae*. *Applied and Environmental Microbiology*, 85(15). https://doi.org/10.1128/AEM.00551-19

Wang, L., Zhao, X. Q., Xue, C., & Bai, F. W. (2013). Impact of osmotic stress and ethanol inhibition in yeast cells on process oscillation associated with continuous very-high-gravity ethanol fermentation. *Biotechnology for Biofuels*, 6(1), 133. https://doi.org/10.1186/1754-6834-6-133

Zheng, L., Liu, M. Q., Sun, J. D., Wu, B., & He, B. F. (2017). Sodium ions activated phosphofructokinase leading to enhanced D-lactic acid production by *Sporolactobacillus inulinus* using sodium hydroxide as a neutralizing agent. *Applied Microbiology and Biotechnology*, 101(9), 3677–3687. https://doi.org/10.1007/s00253-017-8120-0

## SUPPORTING INFORMATION

Additional Supporting Information may be found online in the supporting information tab for this article.

---